Available online at www.sciencedirect.com
SCIENCE DIRECT®
International Journal of Solids and Structures 42 (2005) 759–769
INTERNATIONAL JOURNAL OF SOLIDS and STRUCTURES
www.elsevier.com/locate/ijsolstr

Thermal fatigue crack networks parameters and stability: an experimental study

V. Maillot [a,*], A. Fissolo [b], G. Degallaix [c], S. Degallaix [c]

[a] DMN/SRMA, CEA Saclay, 91191 Gif sur Yvette Cédex, France
[b] DM2S/ SEMT, CEA Saclay, 91191 Gif sur Yvette Cédex, France
[c] Ecole Centrale de Lille, Cité Scientifique BP 48, 59651 Villeneuve d'Ascq, France

Received 28 May 2004
Available online 11 August 2004

Abstract

A thermal fatigue device—called SPLASH—similar to the facility developed by Marsh [Fatigue crack initiation and propagation in stainless steels subjected to thermal cycling, International Conference on Mechanical Behaviour and Nuclear Applications of Stainless Steels at Elevated Temperature, 1981] has been built in CEA/SRMA in 1985. Since then, it was used mostly on austenitic stainless steels to assess the initiation and growth of thermal fatigue crack networks. In 1998, a leak appeared in an auxiliary loop of the primary circuit of a pressurized water nuclear plant in Civaux (France). Thermal fatigue was suspected and studies began on AISI 304 L type austenitic stainless steel. They were eventually compared to results obtained earlier on AISI 316 L(N). First, the initiation conditions were determined and the damage before initiation was qualitatively observed. Then, some crack networks parameters were chosen and quantitatively determined by image analysis. This part of the study was done at the surface, during crack growth, and at the end of the tests, in depth. Finally, the stability of the crack networks obtained by thermal fatigue was tested under isothermal load controlled four point bending fatigue test, and some conclusions were drawn on the mechanisms of propagating crack selection.

Keywords: Thermal fatigue; Crack networks; Initiation; Propagation; Stability; 304 L

* Corresponding author. Tel.: +33 1 69 08 39 43; fax: +33 1 69 08 71 30.
E-mail address: valerie.maillot@cea.fr (V. Maillot).

0020-7683/$ - see front matter © 2004 Elsevier Ltd. All rights reserved.
doi:10.1016/j.ijsolstr.2004.06.032

1. Introduction

Thermal fatigue induces in-service damage in moulds, rolling mill cylinders or turbine blades for instance (Burlet et al., 1990). It also occurs in nuclear reactor components: in as early as 1960, it was observed at Los Alamos. In LMFBRs (liquid metal fast breeder reactors), the mixing of sodium flows at different temperatures or the movement of sodium stratification interface sometimes result in thermal fatigue damage (Gelineau et al., 1994). In PWRs (pressurized water reactors), crack networks may appear in auxiliary loops, next to a cold-water injection site, in spite of relatively small temperature fluctuations (Crutzen et al., 1994, Cipière and Le Duff, 2001). The present study focused on the crack initiation conditions, and on the determination of quantitative parameters of crack networks development under thermal fatigue loading. It is usually assumed that thermal fatigue cracks do not propagate a lot in depth. This point was investigated. It is also usually assumed that an additional mechanical (and isothermal) loading could appear and solicit the already existing crack networks. To investigate the crack networks stability under such a solicitation, an isothermal load controlled four point bending fatigue test was performed on crack networks: the propagation mechanisms and the importance of shielding effects between cracks were thus experimentally observed.

2. Experimental procedures

The steels studied here are 304 L (mostly) and 316 L(N) (for comparison purposes only) type austenitic stainless steel. The 304 L type steel was supplied in sheet of 30 mm thickness and solution-treated for 1 h at 1050 °C and then water-quenched. It presents a grain size of 50 μm and a δ-ferrite content of 1 (in surface) to 4% (in bulk). The chemical compositions are given in Table 1.

2.1. Thermal fatigue tests

In in-service components, thermo-mechanical loading usually results from temperature gradients in thickness. The SPLASH facility described in Fig. 1 is a quasi-structure device, and reproduces this kind of gradients. The specimen geometry is parallelepipedic ($240 \times 20 \times 30$ mm^3). It is continuously heated by Joule effect at the maximum temperature T_{max}, and cyclically submitted to thermal down-shocks by water sprays on two opposite sides, until the chosen minimum temperature T_{min} is reached on the external surfaces The dimensions of the as-treated surfaces are about 30×9 mm^2. Thermo-mechanical loading comes from temperature gradients in the specimen thickness. Fig. 2 presents, as an example, the results of a test performed in the temperature range [175–325 °C]. The duration of the thermal cycle was 7.75 s, with 0.25 s for cooling and 7.5 s for heating.

The earlier studies were performed in LMFBR conditions, Fissolo et al. (1996) and the on going study is performed on PWR conditions. Loading conditions are described in Table 2.

In PWR conditions, nine tests were performed on 304 L type steel and one on 316 L(N), with $T_{max} = 320$ °C. The main objective being the temperature range [T_{min}–T_{max}] of 150 °C, six tests on 304 L and the test on

Table 1
Chemical composition (wt %) of 304 L and 316 LN steels

	C	Mn	Si	Cr	Ni	Mo	S	P	Cu	Al	B	N	Fe
304 L	0.031	1.48	0.55	19.4	8.6	0.23	0.003	0.028	0.17	0.025	0.0015	0.058	Bal.
316 LN	0.024	1.82	0.46	17.44	12.33	2.3	0.001	0.003	0.2		0.0008	0.06	Bal.

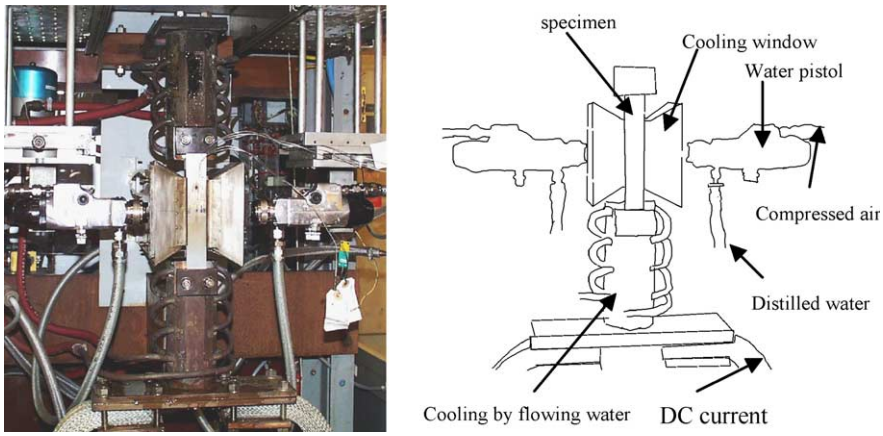

Fig. 1. SPLASH device.

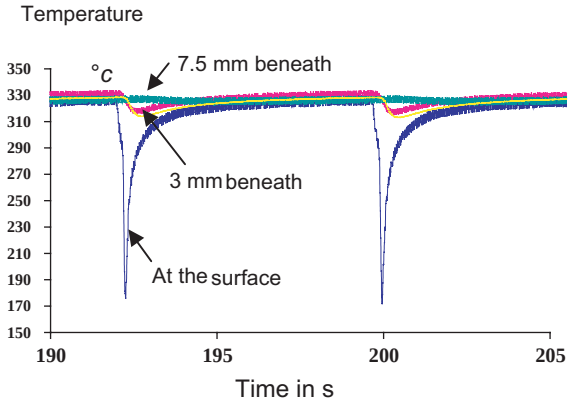

Fig. 2. Temperature variation at different depths.

Table 2
Loading conditions

Conditions	Steel type	Maximum temperature (°C)	Temperature range (°C)
LMFBR	316 L(N)	550	Between 100 and 300
PWR	304 L and 316 L(N)	320	150 or 200

316 (L)N were carried out under these conditions, interrupted respectively at the following chosen number of cycles: 60 000, 300 000 (two tests), 350 000, 500 000 and 700 000 cycles. Two tests were conducted with $\Delta T = 200$ °C, up to 150 000 and 300 000 cycles, and one with $\Delta T = 125$ °C, up to 500 000 cycles, in order to evaluate the temperature range effect.

Before testing, the specimens were carefully polished. The tests were regularly interrupted in order to allow observation of the lateral surfaces by optical microscopy: every 10 000 cycles before initiation (conventionally defined as the presence of at least one 100 μm length crack at the surface), and every 25 000 cycles after. After 50 000 cycles, a very slight mechanical oxide removing is performed on the quenching

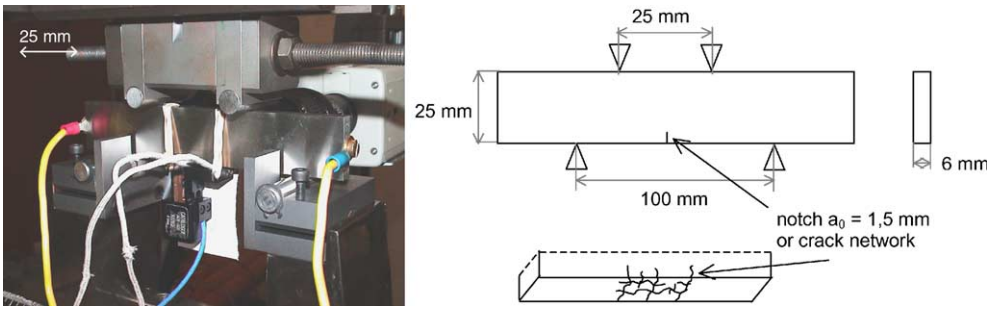

Fig. 3. Four point bending fatigue test device and specimen geometry.

zone. For one test, the observations before initiation were carried out every 1000 cycles in order to detect the surface relief initiating micro cracks. Before initiation, slip systems are activated and intensify during the cycling. Cracks initiate either on slip bands or on surface defects (Fig. 3).

At the end of the tests, as two cracking networks were obtained on the specimen, the in-depth development of one of them was studied (except for the $\Delta T = 125$ °C-specimen), thanks to a step-by-step polishing, removing thin layers of about 100 μm. The second network was kept for further experiments. The at-the-surface extension of the crack networks during the tests, as well as its in-depth development, were studied using image analysis software APHELION; needing manual retranscriptions of the observed networks.

2.2. Stability of crack networks under additional mechanical loading

Isothermal four point bending fatigue tests were performed on a 100 kN-hydraulic INSTRON machine (Fig. 8), at room temperature and under load control ($R_p = 0.1$). The specimen geometry was parallelepipedic ($6 \times 25 \times 140$ mm^3). Two types of specimens were used. The first type specimens were machined in SPLASH specimens, the thermal-fatigue crack-network being situated on the bottom face. The second type presented a machined single notch, with an initial length of 1.5 mm. Six specimens with crack networks were tested, and three with a notch. In all specimens with crack networks, at least one crack was deeper than 1.5 mm.

The crack propagation on the ahead face was followed thanks to a video camera during the fatigue tests. The idea was to compare the propagation of the cracks of a network to that of a single crack initiating at the notch tip.

3. Thermal fatigue results

3.1. Damage prior initiation

In PWRs conditions, before initiation, slip marks appear very rapidly at the surface. The activated slip systems, first single then multiple, strongly intensified with the cycling (Fig. 4a or b). For $\Delta T = 150$ °C for instance, a significant evolution can be detected a long time before the conventional initiation. A very intense gliding is clearly evidenced on surface after only 1000 thermal cycles, whereas first 50 μm crack is detected after 70 000 cycles. Generalisation of the intense gliding is progressively observed. Note that such evolution is the same for isothermal fatigue (Suresh, 1992). Slip bands can cross over the major barriers, such as grain boundaries or twins (Fig. 4c).

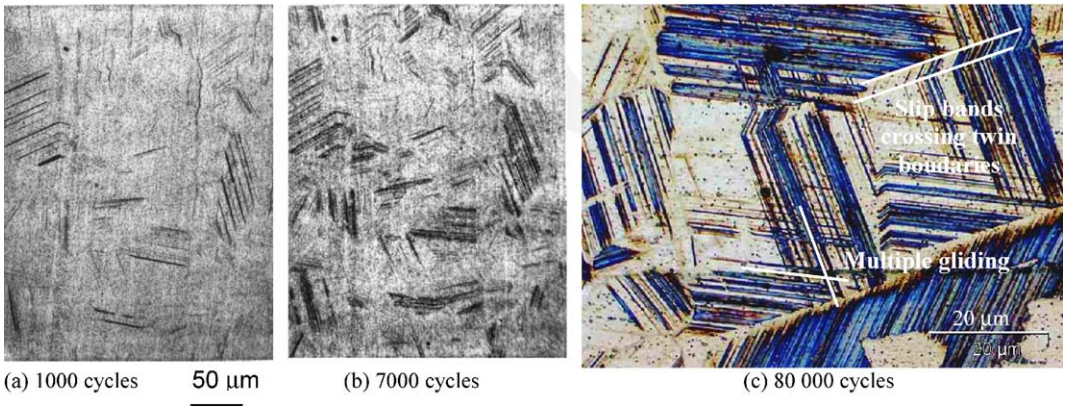

Fig. 4. Gliding intensification during cycling; multiple gliding and crossing over boundaries $T_{max} = 320$ °C, $\Delta T = 150$ °C, 304 L (optical microscopy images).

3.2. Initiation

First of all it should be noted that whatever the material or the experimental conditions, initiation is always multiple, a number of cracks appearing simultaneously on the specimen surface. Cracks are detected by optical microscopy, when they have a 50–150 mm surface length. Initiation occurs on well-developed slip bands or also on punctual defects at the surface (Fig. 5). For a given maximal temperature, the number of cycles to initiation is strongly influenced by the temperature range. For $T_{max} = 320$ °C, it is comprised between 70 000 and 90 000 for the temperature range of 150 °C (for both 304 L and 316 L(N)), between 50 000 and 60 000 for 200 °C, and corresponds to 190 000 for 125 °C. In LMFBR conditions, the initiation can occur much sooner: less than 100 000 cycles for $T_{max} = 550$ °C and $\Delta T = 250$ °C (Fig. 6).

3.3. Propagation

At the surface, there is a strong difference between LMFBR and PWR conditions. In LMFBR conditions, a lot of cracks appear almost simultaneously and the network seems to 'stabilize'—as far as the number of cracks and their lengths are concerned—very quickly. On the contrary in PWR conditions, the crack networks develop slowly (Fig. 7). In LMFBR conditions, the crack density (defined as the cracked length per cracked area) is high. It is not the case in PWR conditions (Fig. 7 compared to Fig. 8).

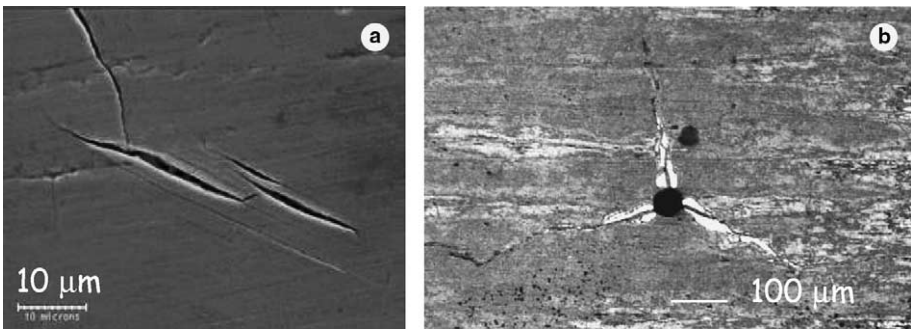

Fig. 5. SEM images: (a) initiation on slip bands and (b) initiation on surface defects.

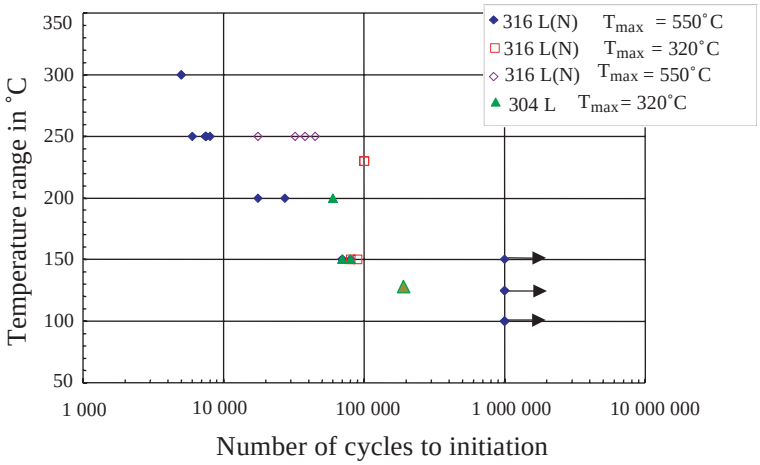

Fig. 6. Temperature range vs. number of cycles to initiation.

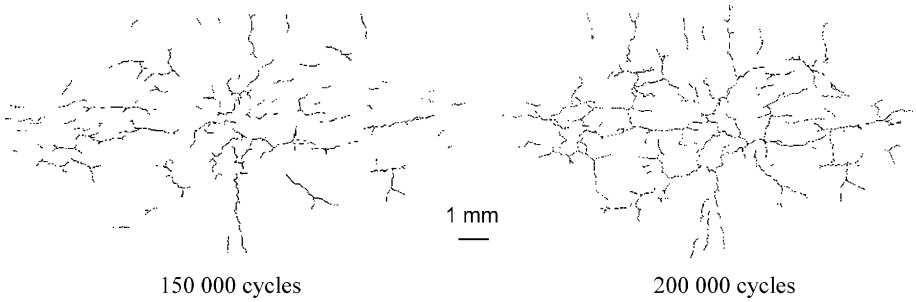

Fig. 7. Extension of crack network at the surface, 304 L, PWR condition, $T_{max} = 320$ °C, $\Delta T = 150$ °C.

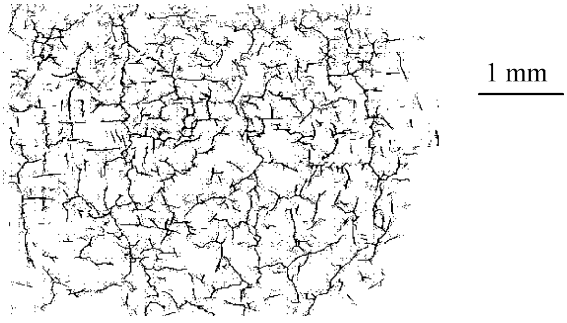

Fig. 8. 316 (N), LMFBR conditions, $T_{max} = 550$ °C, $\Delta T = 150$ °C, after 20 000 cycles.

In depth, in PWR conditions, the crack density falls down very quickly. Only a few cracks remain at 1 mm below the surface (Fig. 9).

In PWR conditions, different geometrical parameters were defined in order to characterize quantitatively the network morphology by image analysis, at the surface (development during cycling) as well as in-depth (at the end of the test). Three parameters are presented in this paper.

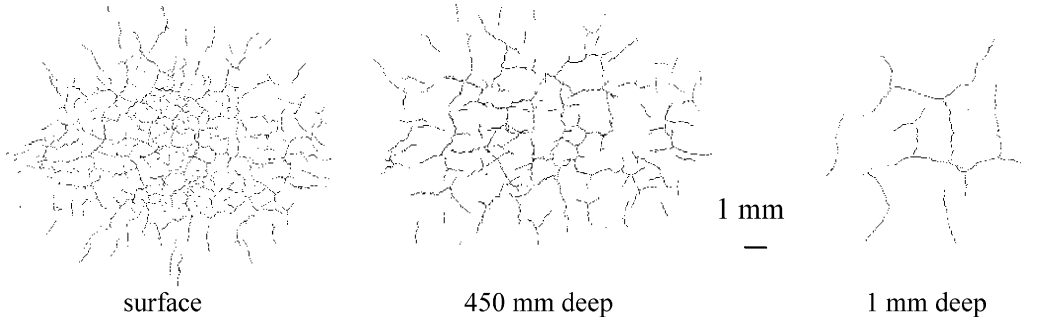

Fig. 9. 304 L, PWR conditions, $T_{max} = 320$ °C, $\Delta T = 200$ °C, after 150000 cycles.

Fig. 10 shows the evolution of the total crack-length at the surface with the number of cycles. Despite the experimental scatter, this parameter is quasi-proportional to the number of cycles, at least up to 400000 cycles; its stabilization is observed above 450000 cycles for the temperature range $\Delta T = 150$ °C. Moreover, the total crack-length increases with the temperature range. There is a very slight influence of the steel grade (316 L(N) vs. 304 L).

Fig. 11 presents the evolution of the crack density at the surface with the number of cycles. The crack density is defined as the ratio of the total crack-length to the crack-network area. Despite the relatively large scatter, this parameter seems only slightly affected by the number of cycles, and not affected by either the temperature range or the steel grade. It can be explained by a balance between extension of the cracked area and crack densification. On the contrary, if the crack density is evaluated on the central network area (the network area at 200000 cycles taken as a reference), the crack density is proportional to the number of cycles up to 400 000 cycles, then the crack network stabilizes (Fig. 12).

Fig. 13 gives the evolution of the total crack-length with the depth for three tests stopped at 150000 cycles (two with $\Delta T = 150$ °C and one with $\Delta T = 200$ °C) and another test stopped at 300000 cycles (with $\Delta T = 200$ °C). Despite a factor-3 scatter band, the curves corresponding to the three first tests are

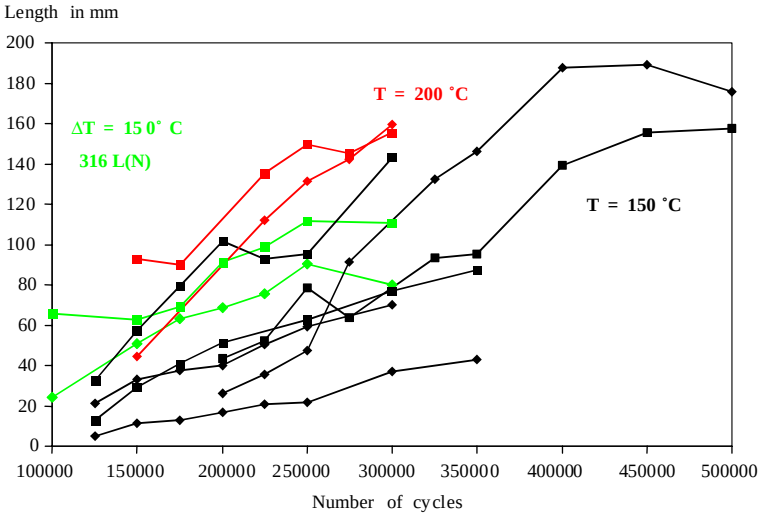

Fig. 10. Evolution of the total crack-length at the surface with the number of cycles.

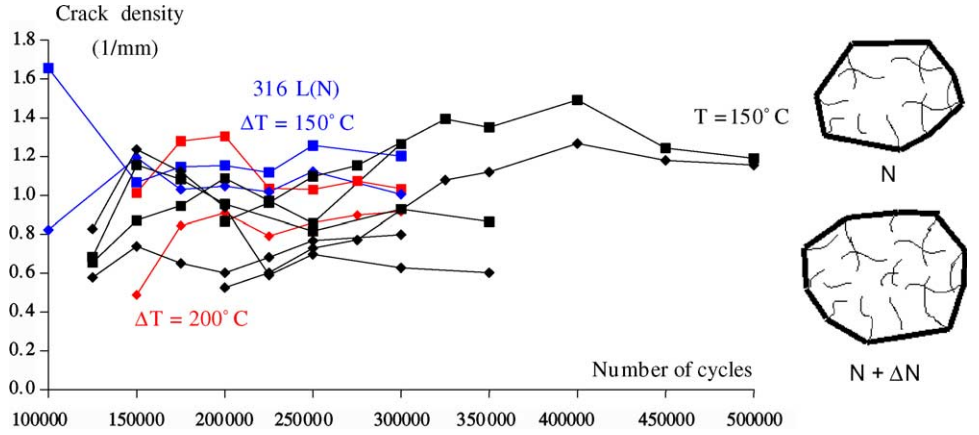

Fig. 11. Evolution of the crack density at the surface with the number of cycles.

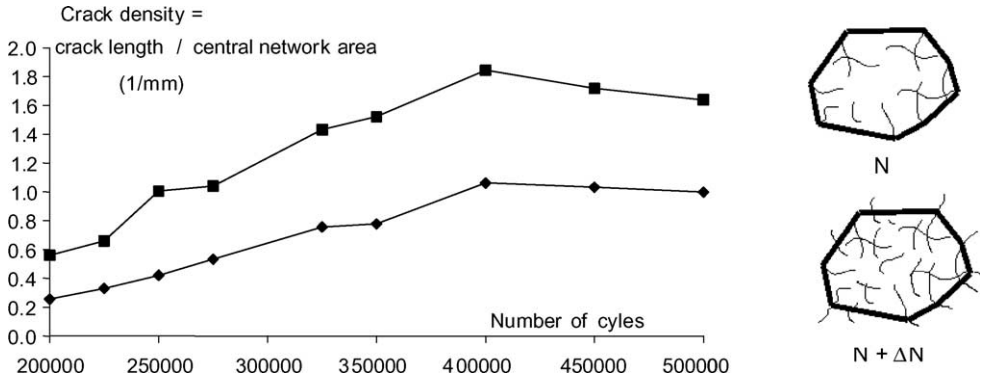

Fig. 12. Evolution of the crack density defined by crack length/central network area at the surface with the number of cycles.

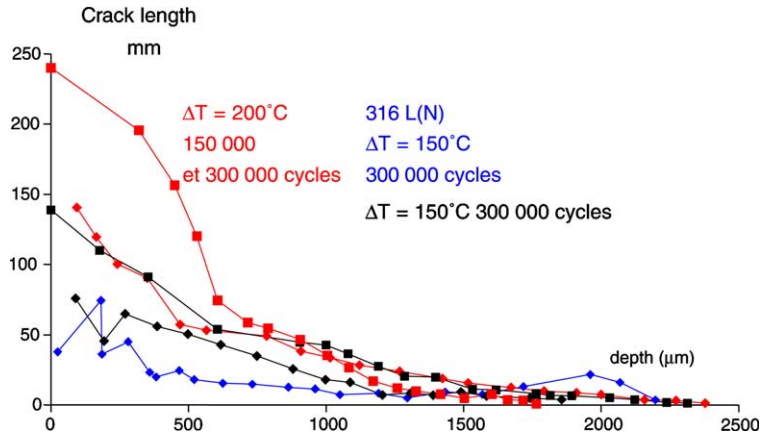

Fig. 13. Evolution of the crack density defined by crack length/central network area at the surface with the number of cycles.

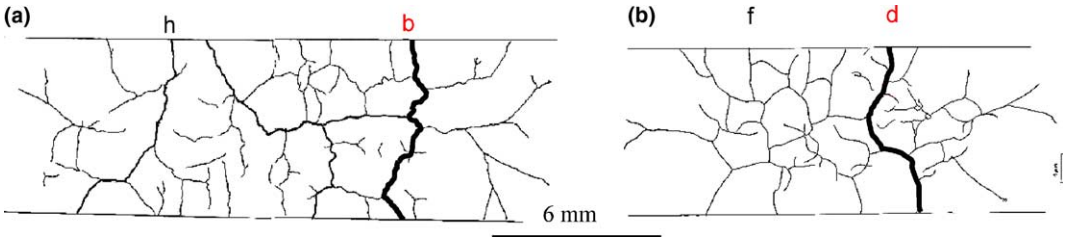

Fig. 14. Thermal fatigue networks ($\Delta T = 150$ °C: (a) 500 000 cycles; (b) 700 000 cycles) tested in four point bending fatigue (ahead face is down).

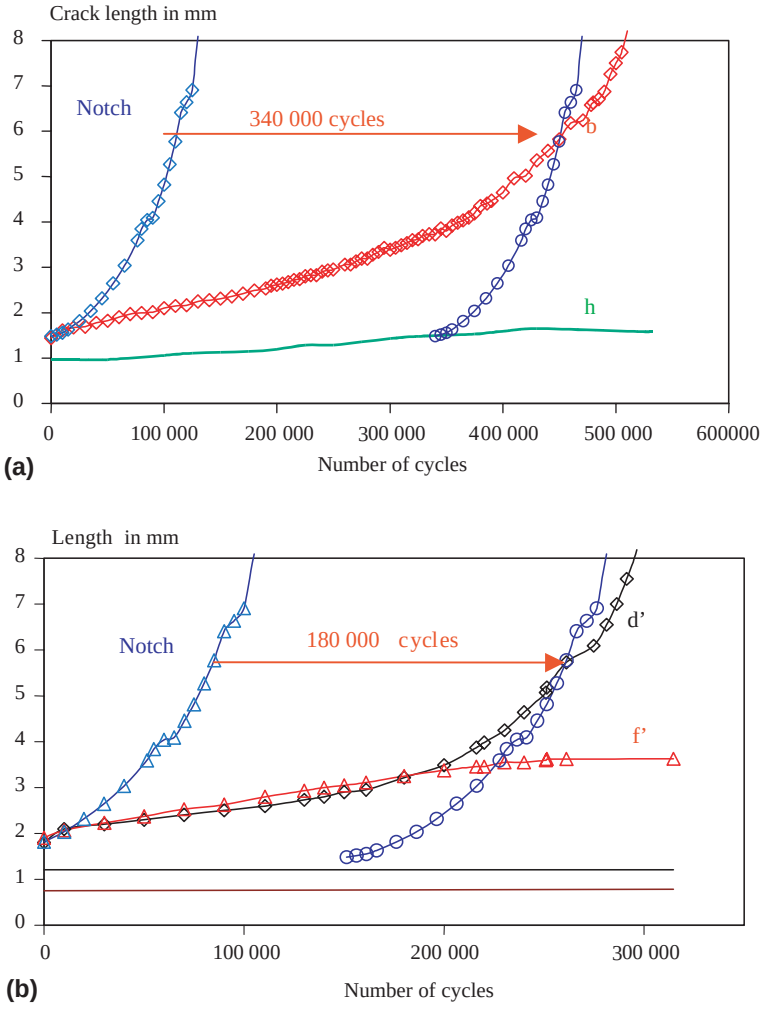

Fig. 15. Crack propagation in four point bending-fatigue of the dominating crack of a network ($\Delta T = 150$ °C: (a) 500 000 cycles; (b) 700 000 cycles). Comparison with propagation of a single crack initiated at the notch tip.

comparable. The fourth curve shows that a double number of cycles leads approximately to a double total crack-length, but only to a depth of about 1 mm. After 1 mm in depth, the four curves are very similar,

corresponding to slight crack networks in a reduced central zone. Whatever the test performed with $\Delta T = 150$ or 200 °C—on 316 L(N) or on 304 L type steel-, the maximum depth of the network never exceeds 2.5 mm, even if in some cases this depth was reached after only 300 000 cycles. In the case of the test performed with $\Delta T = 125$ °C and stopped after 500 000 cycles, the maximum depth was only 1.3 mm.

4. Stability of crack networks under additional mechanical loading results

Fig. 14 shows the thermal crack-networks present on the bottom face of two specimens before testing. They correspond to SPLASH specimens tested in PWR condition on 304 L type steel, with $\Delta T = 150$ °C respectively during 500 000 and 700 000 cycles. In the case of the first network, nine cracks emerge on the ahead face while only four in the case of the second network.

During four point fatigue testing, the camera observations lead to define two stages.

The first stage corresponds to mechanisms of selection of a dominating crack, among all the cracks of the network. By shielding effect due to longest neighbours, some cracks do not propagate at all or only scarcely. A severe competition is generally observed between two cracks, situated rather on the periphery of the network. The crack becoming dominant (the crack b in Fig. 14a; the crack d in Fig. 14b, marked by bold lines in the drawing) is not necessarily the deepest at the beginning of the test, but that presenting less branching on the bottom face or a less tortuous path.

The second stage begins when the selection mechanisms of the dominating crack are achieved. Then, only the dominating crack continues to propagate, all the others being definitively stopped by shielding effects. Progressively, its crack-growth rate gets closer to the one of a single crack initiated at the notch tip. As shown in Fig. 15, the comparison between the length of the dominating crack and the length of a single crack shows a significant delay effect. In the present case, this delay corresponds, respectively, to 340 000 and 180 000 cycles for a 6 mm length.

5. Conclusions

The thermal fatigue conditions (LMFBR or PWR) strongly affects the number of cycles to initiation, as well as the network morphology: the LMFBR conditions lead quickly to a very dense crack network.

For a given T_{max}, the highest the temperature range, the quickest the initiation. The initiation occurs along gliding lines or on small defects.

In PWR conditions, the maximal crack depth obtained is 2.5 mm. The networks stabilize on the surface (in terms of crack length or of crack density) after 400 000 cycles for $\Delta T = 150$ °C. The morphological parameters obtained by image analysis constitute a data base for comparison to cracks networks obtained in in-service conditions.

Under an additional isothermal mechanical loading, one or more cracks from the network can propagate. All cracks but one stop, because of shielding effects between cracks. The propagation of the remaining crack follows the same crack growth rate as the single crack initiated at a notch tip. Under load controlled mechanical loading, the existence of a crack network induce a delay in the propagation. This delay depends on the network morphology.

Acknowledgment

The authors wish to thank Y. Meyzaud and J.A. Le Duff (Framatome ANP), J. C. Le Roux, J. M. Stephan and C. Amzallag (EDF) for support to the ongoing research program.

References

Burlet, H., Vasseur, S., Cailletaud, G., Pineau, A., 1990. Fatigue crack under thermomechanical loading Application to life prediction of centrifugal equipment, EGF 6.

Cipière, M.F., J.A., Le Duff, J.A., 2001. Thermal fatigue experience in French piping. International Institute of Welding, Document no. XIII-1891-01, Lubjana.

Crutzen, S., Birac, C., Champigny, F., Dugué, C., Benoist, P., 1994. Fontevraud 3 1, 12–16.

Fissolo, A., Marini, B., Nais, G., Wident, P., 1996. Thermal Fatigue Behaviour for a 316L Type Steel. J. Nucl. Mater. 233–237, 156–161.

Gelineau, O., Speriando, M., Martin, P., Ricard, J.B., Bougault, A., 1994. Thermal fluctuation problems encountered in LMFRs. Aix en Provence.

Marsh, D.J., 1981. Fatigue crack initiation and propagation in stainless steels subjected to thermal cycling. In: International Conference on Mechanical Behaviour and Nuclear Applications of Stainless Steels at Elevated Temperature.

Suresh, S., 1992. Fatigue of Materials, Cambridge Solid State Sciences Series. Cambridge University Press.